Comparison Between Bulk and FDSOI POM Flash Cell: A Multiscale Simulation Study

Vihar P. Georgiev, Salvatore Maria Amoroso, *Member, IEEE*, Talib Mahmood Ali, Laia Vilà-Nadal, Christoph Busche, Leroy Cronin, and Asen Asenov, *Fellow, IEEE*

***Abstract*— In this brief, we present a multiscale simulation study of a fully depleted silicon-on-insulator (FDSOI) nonvolatile memory cell based on *polyoxometalates* (POMs) inorganic molecular clusters used as a storage media embedded in the gate dielectric of flash cells. In particular, we focus our discussion on the threshold voltage variability introduced by random discrete dopants (random dopant fluctuation) and by fluctuations in the distribution of the POM molecules in the storage media (POM fluctuation). To highlight the advantages of the FDSOI POM flash cell, we provide a comparison with an equivalent cell based on conventional (BULK) transistors. The presented simulation framework and methodology is transferrable to flash cells based on alternative molecules used as a storage media.**

***Index Terms*— Device variability, molecular electronics, multiscale modeling, nonvolatile memory (NVM), polyoxometalates (POM).**

I. Introduction

OVER the last couple of decades, flash cells have undergone aggressive scaling reaching the 15-nm half-pitch (F) mark. This has been accompanied by scaling of a tunnel oxide thickness to improve the programming/erasing performance. At the same time, an interpoly dielectric thickness has been reduced to keep the capacitance coupling ratio at an almost constant value to achieve acceptable ratios between the control and floating gate (FG) voltages [1]. However, further scaling of the current NAND flash memory cells faces significant challenges including: 1) strong coupling between FGs in neighboring cells [2]; 2) charge loss from the FG [3]; and 3) random dopant fluctuations (RDF) that induce variability in flash cells [4].

Nanoscrystals and charge-trapping memories have been proposed aiming to improve the flash cell performance [5], [6].

Manuscript received May 19, 2014; revised October 26, 2014; accepted December 1, 2014. Date of publication December 23, 2014; date of current version January 20, 2015. This work was supported by the U.K. Engineering and Physical Sciences Research Council Platform under Grant EP/H024107/1 through the Project entitled Molecular-Metal-Oxide-nanoelectronicS: Achieving the Molecular Limit. The review of this brief was arranged by Editor Y.-H. Shih.

V. P. Georgiev, S. M. Amoroso, and T. M. Ali are with the Device Modelling Group, School of Engineering, University of Glasgow, Glasgow G12 8QQ, U.K. (e-mail: vihar.georgiev@glasgow.ac.uk; salvatore.amoroso@glasgow.ac.uk; t.ali.1@research.gla.ac.uk).

L. Vilà-Nadal, C. Busche, and L. Cronin are with Westchem, School of Chemistry, University of Glasgow, Glasgow G12 8QQ, U.K. (e-mail: laiavn@chem.gla.ac.uk; Christoph.Busche@glasgow.ac.uk; lee.cronin@glasgow.ac.uk).

A. Asenov is with the Device Modelling Group, School of Engineering, University of Glasgow, Glasgow G12 8QQ, U.K., and also with Gold Standart Simulations Ltd., Glasgow G12 8LT, U.K. (e-mail: asen.asenov@glasgow.ac.uk).

Color versions of one or more of the figures in this paper are available online at http://ieeexplore.ieee.org.

Digital Object Identifier 10.1109/TED.2014.2378378

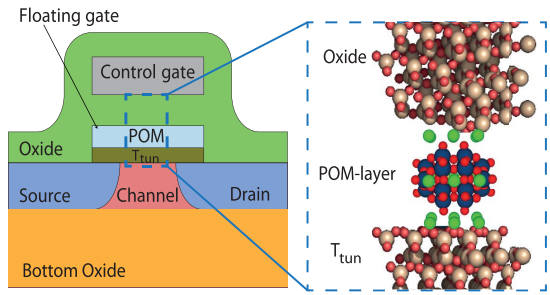

Fig. 1. Schematic of a single-transistor FDSOI memory cell, indicating the aimed substitution of the poly-Si FG with an array of POM molecules (POM layer). Legend: W—blue, O—red, Si—brown, and point charges representing the surrounding counter cations—green.

However, the random number and position of the traps create a significant additional variability in the threshold voltage of the programmed flash cells [7], [8]. One possible option for an improvement is to replace the nanocrystals/random defects with molecules [9], [10]. Among the possible candidates are polyoxometalate (POM) molecules, metal oxide clusters, where the metal atoms are usually group 5 or group 6 transition metals (W, Mo, ...) in their highest oxidation state [11], [12]. POMs have attractive properties for potential nonvolatile memory (NVM) application due to their ability to undergo stable, multiple, and reversible oxidation/reduction processes. Moreover, the embedding of numerous types of POMs with SiO_2 has been experimentally demonstrated as advantageous for the NVM application [13], [14]. This, in combination with the self-assembly of the POMs, is expected to yield a low-voltage threshold (V_T) variability.

To explore the full potential and POM-based flash cell technology, we compare multiscale computational simulations of fully depleted silicon-on-insulator (FDSOI) and conventional (BULK) POM flash memory cells. In addition, we provide a comparison with new and some of the previously reported results of the simulation of the BULK POM flash memory cell [15], [16]. Extensive information about the cell design and the simulations methodology is available in [16].

II. FDSOI Versus BULK Flash Cell Performance

Fig. 1 reveals the schematic of a single POM based on the FDSOI flash cell. In this section, we benchmark the behavior of the FDSOI POM flash cell against the BULK cell result. The main focus is on the programming window (ΔV_T) and I_D–V_G characteristics of smooth devices with continuous doping. In the simulations, each smooth transistor has

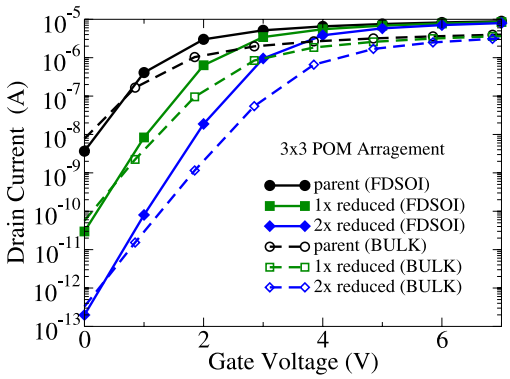

Fig. 2. I_D–V_G for the BULK and FDSOI flash cell smooth devices—*parent* $[W_{18}O_{54}(SO_3)_2]^{4-}$, *1x reduced* $[W_{18}O_{54}(SO_3)_2]^{5-}$, and *2x reduced* $[W_{18}O_{54}(SO_3)_2]^{6-}$. Inner part—potential profile of nine POMs arranged in a 3×3 regular grid in the FG.

nine POMs placed in a perfect grid in the FG. The distance between the POMs molecules is 3 nm to exclude physical overlap between the two structures, which is in agreement with the experiments [13], [14]. The total oxide (SiO_2) thickness is 20 nm, including the POMs layer (Fig. 1). The tunneling oxide (T_{tun}) is 4.5 nm (3-nm high-quality SiO_2 and 1.5-nm POMs layer), the bottom oxide is 15-nm thick, and the entire gate-stack is identical to our previously published work [16].

To investigate the device performance, we consider the $[W_{18}O_{54}(SO_3)_2]^{n-}$ POM cluster as a charge storage center, having three easily accessible redox states. These are the *parent* ($n = 4$), *1x reduced* ($n = 5$), and *2x reduced* ($n = 6$) states. The *parent* flash cell has zero total charge in the FG because, even though the nine $[W_{18}O_{54}(SO_3)_2]^{4-}$ POMs are negatively charged, their charge is neutralized by the positively charged cations, which are represented by point charges in our simulations (Fig. 1). In the case of the *1x reduced* NVM cell, the total amount of charges in the FG is -9 q (q—unit charge of electron). Correspondingly, the *2x reduced* transistors have -18 q in comparison with the *parent* structure.

The related I_D–V_G characteristics for the FDSOI and BULK cells are shown in Fig. 2. All characteristics are aligned in order for the *parent* structures of the FDSOI and BULK transistors to have identical V_T determined by a current criterion of the 10^{-7} A drain current (black curves in Fig. 2 intersect at drain current $= 10^{-7}$ A). Several important observations can be made from the data presented.

First, because the short-channel effects are less pronounced in the FDSOI cell in comparison with the BULK flash cell, the FDSOI cell has lower leakage current, higher drive current, and steeper subthreshold slope in comparison with the BULK devices.

Second, our calculations show a reduction of threshold voltage shift (ΔV_T) between the *parent*, *1x reduced*, and *2x reduced* configurations for the FDSOI devices in comparison with the BULK cells. Narrowing of ΔV_T between discussed states in FDSOI, if compared with the BULK cell, is clearly visible in Fig. 3. Fig. 3 also compares the analytical results of ΔV_T versus Q_S, obtained from the sheet-charge approximation (SCA), with the results from the 3-D simulations. The values of ΔV_T for transition from the *parent* to *1x reduced* state are 1.17 and 0.95 V for the BULK and FDSOI structures correspondingly. In the case of transition from the *1x reduced* to *2x reduced* state for the BULK transistor, the value is 1.16 V and for the FDSOI structure it is 0.84 V.

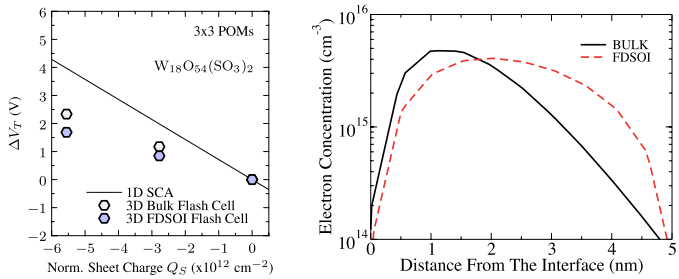

Fig. 3. Left—dependence of the threshold shift ΔV_T on the sheet density of POM. Analytical solution based on an SCA is shown for comparison. Symbols indicate charges corresponding to the 3×3 arrangements of POMs, for the *parent*, *1x reduced*, and *2x reduced* $[W_{18}O_{54}(SO_3)_2]^{n-}$. Right—1-D electron density profile at V_T in the middle of the channel for the two FDSOI and BULK POM flash cell architectures.

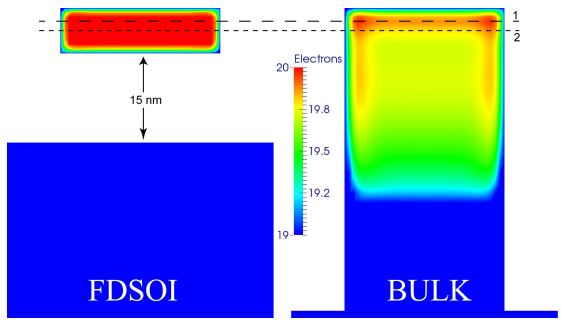

Fig. 4. Electron density at V_T in the channel, vertical cut along width (center of the channel) of the FDSOI (left-hand side) and BULK (right-hand side). The dashed lines 1 and 2 represent the charge centroid for the BULK and FDSOI devices correspondingly. Please note that the oxide is cut away.

The right-hand side of Figs. 3 and 4 reveals the charge distribution in the middle of the channel for the BULK and FDSOI structures. The plot in Fig. 3 shows that the maximum of the 1-D electron density distribution in the channel is farther away from the surface in the FDSOI devices in comparison with the BULK structures. This is also visible in Fig. 4, where the dashed lines represent the charge centroids for the FDSOI and BULK structures. Due to the fact that the charge for the FDSOI transistor is farther from the Si/SiO_2 interface in comparison with the BULK device, the influence of a trapped charge in the FG on the V_T shift is smaller. Hence, the current flow through the channel in the FDSOI case is less disturbed by the number and the position of the POMs in the FG in comparison with the BULK structure.

Having established that the FDSOI cell has better I_D–V_G characteristics with narrowing of ΔV_T window if compared with the BULK cell, it is important to investigate how sources of statistical variability (SV) determine the V_T distribution in the FDSOI and the BULK flash cells.

III. Statistical Variability

Consistently with our previous work [16], we introduced two principal sources of SV. The first source of SV (RDF)

TABLE I

NOMINAL THRESHOLD VOLTAGE OF THE BULK CELL WITH THREE STATES AND THE CORRESPONDING AVERAGE AND STANDARD DEVIATION VALUES FOR THE THREE ENSEMBLES WITH VARIABILITY

Bit	**Nominal V_T**	**RDF 2000 devices**		**POMF 2000 devices**		**RDF+POMF 2000 devices**	
Redox state	V_T	μV_T	σV_T	μV_T	σV_T	μV_T	σV_T
	(V)	(V)	(mV)	(V)	(mV)	(V)	(mV)
(1) parent	1.778	1.821	448	1.778	0	1.820	449
(2) 1x red.	2.948	2.976	443	2.945	42	2.974	446
(3) 2x red.	4.107	4.122	437	4.089	91	4.113	453

TABLE II

NOMINAL THRESHOLD VOLTAGE OF THE FDSOI CELL WITH THREE STATES AND THE CORRESPONDING AVERAGE AND STANDARD DEVIATION VALUES FOR THE THREE ENSEMBLES WITH VARIABILITY

Bit	**Nominal V_T**	**RDF 2000 devices**		**POMF 2000 devices**		**RDF+POMF 2000 devices**	
Redox state	V_T	μV_T	σV_T	μV_T	σV_T	μV_T	σV_T
	(V)	(V)	(mV)	(V)	(mV)	(V)	(mV)
(1) parent	-0.056	-0.052	98	-0.129	0	-0.052	92
(2) 1x red.	0.902	0.784	84	0.716	37	0.786	91
(3) 2x red.	1.743	1.615	77	1.546	73	1.610	105

and it is known to have a dominant impact on their threshold voltage variability [4]. The dopants profile used in the source/drain (S/D) follows the Gaussian distribution. The second source of SV is the random distribution of the position of the POMs in the FG along both the channel length and width, termed POM fluctuations (POMF). Ultimately, both the spatial position and number of the POMs could vary. However, in this brief, we present the results based *only on a constant number of nine* POMs in the FG. The fixed number and relative low number of POM molecules gives us the opportunity to easily establish the relationship between the molecule position in the FG and the behavior of the flash cell.

We consider statistical ensembles of 2000 flash cells each in the statistical numerical device simulations. In the first set of simulations, we analyze the RDF mainly not only in the S/D regions of the FDSOI cell, but also in the channel of the BULK cell. Simultaneously, the nine POMs are arranged in a 3×3 grid in the FG. In the second set of simulations, called POMF, the position of the nine molecules along channel length and width is randomly varied but the flash cells have continuous doping. Finally, in the third set of simulations, marked as RDF + POMF, the combination of the RDF and the random lateral distribution of the position of the nine POMs in the oxide is considered.

In Tables I and II, under the heading *Nominal* V_T, three distinct V_T values for the smooth FDSOI and BULK devices are reported correspondingly. The tables also report the average (μ) and the standard deviation (σ) of the three V_Ts for the simulated ensembles with variability. The corresponding values of V_T are shown in Figs. 5–7 in terms

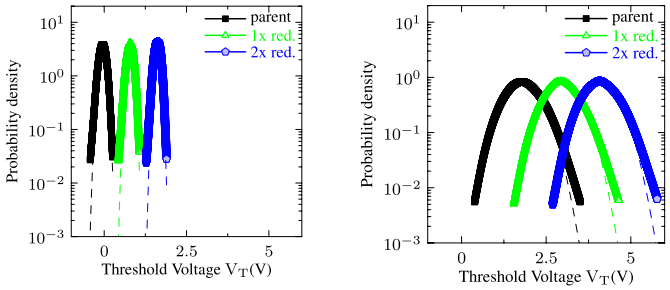

Fig. 5. PDF of the V_T distribution for each state of 2000 FDSOI (left) and BULK (right) flash cells with *RDF only*. Dashed line: Gaussian fit.

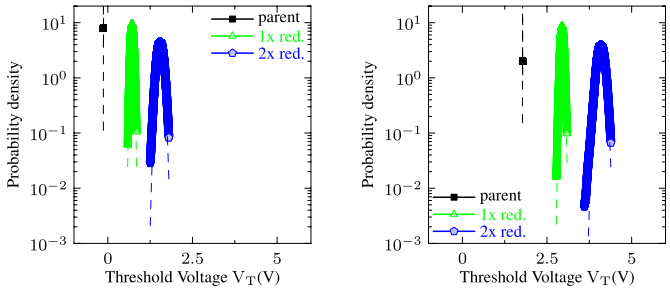

Fig. 6. PDF of the V_T distribution for each state of 2000 FDSOI (left) and BULK (right) flash cells with *POMF only*.

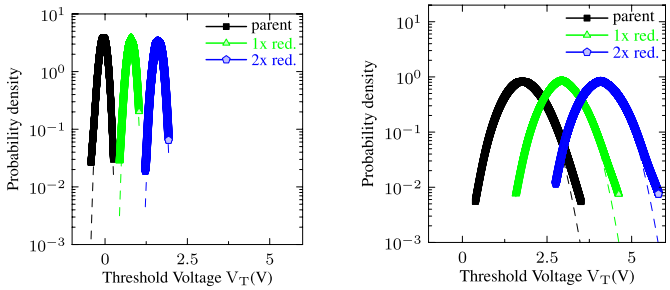

Fig. 7. PDF of the V_T distribution for each state of 2000 FDSOI (left) and BULK (right) flash cells with *RDF + POMF*.

of probability density function (pdf) for each ensemble and each state, comparing the FDSOI and BULK distributions. Based on the presented data, several observations can be made.

First, in the FDSOI case, the nominal (smooth) devices for each bit have lower V_T in comparison with the BULK structures. The average value of V_T for 2000 cells at each bit, for both types of flash cells, is close to the values for the nominal transistors. More importantly, the conclusion established in Section II for the nominal cells, in which the difference between each state in the FDSOI cell is smaller if compared with the BULK transistors, is still valid for μV_T.

Second, the RDF has a dominant impact on the dispersion of V_T in both types of POM-based flash cells, as reflected in the values of σV_T. In addition, σV_T for the RDF ensembles and the RDF + POMF ensembles is almost four times larger in the BULK cells in comparison with the FDSOI case. Moreover, Figs. 5 and 7 reveal that the states in the BULK case overlap significantly even at the value before 1 σ, while in the FDSOI

case, the overlap is almost at 3 σ. Hence, the dispersion of the V_T in the FDSOI case is significantly reduced in comparison with the BULK structure. Another notable feature in the trends of σV_T for the ensembles with RDF is its decrease with the increase of the net negative charge stored in the oxide. This is ascribed to the increasing control of the stored charge over the channel conductance. This effect is more pronounced for the FDSOI cells.

IV. Conclusion

In this brief, we study the nominal and statistical behaviors of the FDSOI and BULK molecular-based flash cells using hierarchical numerical simulations. Two main sources of SV are considered such as RDF and POMF. The results of our analysis highlight that the difference between the threshold voltage shift in the FDSOI structures is smaller in comparison with the BULK case. Second, the FDSOI flash cell has significantly smaller variation of V_T in comparison with the BULK transistor, which indicates a significant potential for high yield at simplified writing scenarios in flash memory applications. However, it is important to point out that device performance depends also on the number of POMs and their organization in the FG. Some initial results have already been presented in our previous work [15] and additional analysis will be reported in the future publications.

References

[1] Y. Noh *et al.*, "A new metal control gate last process (MCGL process) for high performance DC-SF (dual control gate with surrounding floating gate) 3D NAND flash memory," in *Proc. Symp. VLSI Technol.*, Jun. 2012, pp. 19–20.

[2] M. Park, K. Kim, J.-H. Park, and J.-H. Choi, "Direct field effect of neighboring cell transistor on cell-to-cell interference of NAND flash cell arrays," *IEEE Electron Device Lett.*, vol. 30, no. 2, pp. 174–177, Feb. 2009.

[3] S. M. Amoroso, L. Gerrer, F. Adamu-Lema, S. Markov, and A. Asenov, "Impact of statistical variability and 3D electrostatics on post-cycling anomalous charge loss in nanoscale flash memories," in *Proc. IEEE Int. Rel. Phys. Symp. (IRPS)*, Apr. 2013, pp. 3B.4.1–3B.4.6.

[4] A. Ghetti, S. M. Amoroso, A. Mauri, and C. M. Compagnoni, "Impact of nonuniform doping on random telegraph noise in flash memory devices," *IEEE Trans. Electron Devices*, vol. 59, no. 2, pp. 309–315, Feb. 2012.

[5] H.-C. Ma *et al.*, "A novel random telegraph signal method to study program/erase charge lateral spread and retention loss in a SONOS flash memory," *IEEE Trans. Electron Devices*, vol. 58, no. 3, pp. 623–630, Mar. 2011.

[6] T. Shaw, T.-H. Hou, H. Raza, and E. C. Kan, "Statistical metrology of metal nanocrystal memories with 3-D finite-element analysis," *IEEE Trans. Electron Devices*, vol. 56, no. 8, pp. 1729–1735, Aug. 2009.

[7] S. M. Amoroso *et al.*, "3D Monte Carlo simulation of the programming dynamics and their statistical variability in nanoscale charge-trap memories," in *Proc. IEEE Int. Electron Devices Meeting (IEDM)*, Dec. 2010, pp. 22.6.1–22.6.4.

[8] C. Bonafos *et al.*, "Si and Ge nanocrystals for future memory devices," *Mater. Sci. Semicond. Process.*, vol. 15, no. 6, pp. 615–626, Dec. 2012.

[9] H. Zhu *et al.*, "Non-volatile memory with self-assembled ferrocene charge trapping layer," *Appl. Phys. Lett.*, vol. 103, no. 5, pp. 053102-1–053102-4, Jul. 2013.

[10] S. Paydavosi *et al.*, "High-density charge storage on molecular thin films—Candidate materials for high storage capacity memory cells," in *Proc. IEEE Int. Electron Devices Meeting (IEDM)*, vols. 11–543. Dec. 2011, pp. 24.4.1–24.4.4.

[11] N. Fay *et al.*, "Structural, electrochemical, and spectroscopic characterization of a redox pair of sulfite-based polyoxotungstates: α-$[W_{18}O_{54}(SO_3)_2]^{4-}$ and α-$[W_{18}O_{54}(SO_3)_2]^{5-}$," *Inorganic Chem.*, vol. 46, no. 9, pp. 3502–3510, Apr. 2007.

[12] X. López, J. J. Carbó, C. Bo, and J. M. Poblet, "Structure, properties and reactivity of polyoxometalates: A theoretical perspective," *Chem. Soc. Rev.*, vol. 41, no. 22, pp. 7537–7571, 2012.

[13] J. Shaw *et al.*, "Integration of self-assembled redox molecules in flash memory devices," *IEEE Trans. Electron Devices*, vol. 58, no. 3, pp. 826–834, Mar. 2011.

[14] A. M. Douvas, E. Makarona, N. Glezos, P. Argitis, J. A. Mielczarski, and E. Mielczarski, "Polyoxometalate-based layered structures for charge transport control in molecular devices," *ACS Nano*, vol. 2, no. 4, pp. 733–742, Apr. 2008.

[15] L. Vilà-Nadal *et al.*, "Towards polyoxometalate-cluster-based nanoelectronics," *Chem., Eur. J.*, vol. 19, no. 49, pp. 16502–16511, Dec. 2013.

[16] V. P. Georgiev, S. Markov, L. Vilà-Nadal, C. Busche, L. Cronin, and A. Asenov, "Optimization and evaluation of variability in the programming window of a flash cell with molecular metal–oxide storage," *IEEE Trans. Electron Devices*, vol. 61, no. 6, pp. 2019–2026, Jun. 2014.

Vihar P. Georgiev received the Ph.D. degree from the University of Oxford, Oxford, U.K., in 2011.

He joined the Device Modelling Group, School of Engineering, University of Glasgow, Glasgow, U.K., in 2011, where he is currently a Research Associate.

Salvatore Maria Amoroso (S'10–M'12) received the Ph.D. degree in electronic engineering from the Politecnico di Milano, Milan, Italy, in 2012.

He has been an Associate Researcher with the Department of Electronics, University of Glasgow, Glasgow, U.K., since 2012.

Talib Mahmood Ali received the B.Sc. and M.Sc. degrees form the University of Technology at Iraq, Baghdad, Iraq, in 1998 and 2004, respectively. He is currently pursuing the Ph.D. degree with the Device Modelling Group, School of Engineering, University of Glasgow, Glasgow, U.K.

He was a Lecturer with Al-Mustansiriya University, Baghdad, from 2005.

Laia Vilà-Nadal received the Ph.D. degree from Rovira i Virgili University, Tarragona, Spain, in 2011.

She joined the Cronin Group, WestCHEM, School of Chemistry, University of Glasgow, Glasgow, U.K., as a Post-Doctoral Researcher, in 2011.

Christoph Busche received the Ph.D. degree from the Institute of Inorganic Chemistry, University of Heidelberg, Heidelberg, Germany, in 2009.

He has been a member of the Cronin Group with WestCHEM, School of Chemistry, University of Glasgow, Glasgow, U.K., since 2010, as a Post-Doctoral Research Assistant.

Leroy Cronin received the Ph.D. degree in chemistry from the University of York, York, U.K., in 1997. He joined the University of Glasgow, Glasgow, U.K., as a Lecturer in 2002, Reader in 2005, Professor in 2006, Gardiner Professor in 2009, and has been the Regius Professor of Chemistry since 2013. He leads the Complex Chemical Systems Research Group.

Asen Asenov (M'96–SM'05–F'11) received the Ph.D. degree in physics from the Bulgarian Academy of Sciences, Sofia, Bulgaria, in 1989.

He is currently the James Watt Chair of Electrical Engineering with the University of Glasgow, Glasgow, U.K. He is also a Co-Founder and Chief Executive Officer with Gold Standard Simulations Ltd., Glasgow.